Available online at www.sciencedirect.com

ScienceDirect

Journal of the Mechanics and Physics of Solids 55 (2007) 517–532

JOURNAL OF THE MECHANICS AND PHYSICS OF SOLIDS

www.elsevier.com/locate/jmps

Prediction of elastic properties of heterogeneous materials with complex microstructures ☆

Yong Ni, Martin Y.M. Chiang*

Polymers Division, National Institute of Standards and Technology, Gaithersburg, MD 20899-8544, USA

Received 5 April 2006; received in revised form 10 July 2006; accepted 2 September 2006

Abstract

The phase-field microelasticity (PFM) is adapted into a homogenization process to predict all the effective elastic constants of three-dimensional heterogeneous materials with complex microstructures. Comparison between the PFM approach and the Hashin–Shtrikman variational approach is also given. Using 3D images of two-phase heterogeneous media with regular and irregular microstructures, results indicate that the PFM approach can accurately take into account the effects of both elastic anisotropy and inhomogeneity of materials with arbitrary microstructure geometry, such as complex porous media with suspended inclusions.
Published by Elsevier Ltd.

Keywords: Micromechanics; Heterogeneous media; Porous media; Phase-field method; Stiffness

1. Introduction

Heterogeneous media (multiphase materials) are met everywhere in engineering applications. Their structure/property relations are complex and are time consuming to establish experimentally. Consequently, the challenge in using heterogeneous media extends from material design, through microstructure imaging and property predictions, to use limit and lifetime predictions (Christensen, 1979; Sanchez-Palencia and Zaoui, 1987; Nemat-Nasser and Hori, 1993; Torquato, 2002). In this study, we are specifically interested

*Corresponding author. Tel.: +1 301 975 5186; fax: +1 301 975 4924.
E-mail address: martin.chiang@nist.gov (M.Y.M. Chiang).

0022-5096/$ - see front matter Published by Elsevier Ltd.
doi:10.1016/j.jmps.2006.09.001

in the prediction of mechanical properties (elastic constants) of linear elastic heterogeneous materials through a homogenization process, where the material can be idealized as being effectively homogenous in a representative volume element (RVE). The phase-field microelasticity (PFM) model (Wang et al., 2002) is adapted to a homogenization process to estimate all the effective elastic constants of three-dimensional (3D) heterogeneous materials. The PFM, based on the Eshelby effective eigenstrain approach (Eshelby, 1957) and the phase-field theory for attaining the eigenstrain, has been successfully used to calculate the local mechanical fields inside elastic heterogeneous materials (e.g., polycrystals with elastically anisotropic constituent grains). Here we go a step further, aiming at obtaining the entire effective elastic constants without prior knowledge of material symmetry. The heterogeneous media examined in this study are bi-continuous rather than dispersed phase two-phase materials, i.e., an extreme case, porous media having interconnected channel-shaped pores rather than isolated cavities. Various composites with such complex microstructure can be found in practice, for example, the musculoskeletal tissue and bone (Turner et al., 1990; Martin, 1991; Cowin, 1999), porous ceramics (Roberts and Garboczi, 2000), and porous scaffolds for tissue engineering (Hutmacher, 2000; Sun et al., 2005; Hollister, 2005).

The homogenization process is a classic methodology to obtain effective material properties. It treats the heterogeneous media to be a hierarchical mechanical structure with two levels: macro and micro. The material properties at the macro-level (effective material properties) are always assumed as homogeneous and can be obtained through statistical averaging, which takes into account the properties of all phases of the heterogeneous media and their interaction inside the RVE at the micro-level. So far, several rigorous homogenization processes have been developed. Some of them can be categorized as classic micromechanical models, such as the self-consistent method (Hill, 1965; Budiansky, 1965; Christensen and Lo, 1979), the Mori–Tanaka model (Mori and Tanaka, 1973), the differential scheme (McLaughlin, 1977), and the IDD estimate (interaction direct derivative, Zheng and Du, 2001). These models are mainly based on the Eshelby solution for an isolated ellipsoidal inclusion embedded in an infinite medium (Eshelby, 1957) and have adopted different effective-medium approximations to account for the elastic interaction between the inclusions. Other homogenization processes can be categorized as the bounds approach. For example, upper and lower bounds of effective moduli and compliances were firstly obtained based on the rule of mixtures by Voigt and Reuss approximation (e.g., Nemat-Nasser and Hori, 1993). Later, much stronger bounds were derived from the variational principle, known as the Hashin–Shtrikman bounds (Hashin and Shtrikman, 1963; Willis, 1977), and the n-point correlation functions for disordered materials (Kröner, 1977; Torquato, 1997; Torquato, 1998). These bounds serve as benchmarks work to assess the consistency of micromechanical prediction of effective properties, but they are not themselves direct predictions of the effective properties.

Most of homogenization processes in the aforementioned categories have assumed the effective properties to be isotropic. To predict the effective properties of materials possessing macroscopic anisotropy, additional theoretical methods for the homogenization process were proposed with the consideration of spherical inclusions (either rigid or void) embedded in matrix (Nemat-Nasser and Taya, 1981; Nemat-Nasser et al., 1982; Nunan and Keller, 1984; Sangani and Lu, 1987; Kushch, 1987; Cohen, 2004). Numerical methods for the homogenization processes were also proposed with the consideration of inclusions different from spherical shapes, such as the asymptotic method (Sanchez-Palencia and

Zaoui, 1987), the multipole expansion method (Kushch, 1998), the finite element method (Wegner and Gibson, 2000; Kouznetsova et al., 2001), and FFT-based method for composites with linear (Müller, 1996) and nonlinear constituents (Moulinec and Suquet, 1994; Moulinec and Suquet, 1998; Michel et al., 1999; Bilger et al., 2005; Idiart et al., 2006). These methods, which provide the effective properties as well as the values of local stress and strain, were proved to be accurate and effective, but are rarely reported in 3D cases with anisotropy.

In this study, we propose a homogenization process to predict the elastic constants of 3D heterogeneous media, where the microstructure of constituents in the media is highly interconnected and correlated rather than regular or random matrix-inclusion type. Our method is based on the concept of eigenstrain proposed by Eshelby (1957), later developed by Mura (1987). They demonstrated that the elastic strain field and strain energy of a heterogeneous system are identical to those of its equivalent homogeneous system, which is subjected to a *proper* effective eigenstrain field. Therefore, what is critical is to find the proper eigenstrain field for the equivalent homogeneous system. In this study, we adapt the PFM to attain the eigenstrain field and incorporate it into the homogenization process. The results from the study indicate that the effective eigenstrain can be properly found with good computational efficiency for predicting the elastic constants of heterogeneous media, with either isotropic or anisotropic constituents, having arbitrary microstructural geometry and the stiffness contrast between constituents. In the next section, the fundamental theory and necessary equations used in our proposed homogenization process will be illustrated. Comparison between PFM approach and the Hashin–Shtrikman (H–S) variational approach is also presented. Results and discussion on several 3D heterogeneous medium will be given in Section 3.

2. Theory of the method

Let us consider an elastically inhomogeneous solid subjected to an external load. One can find a length scale over which the elastic response of the solid can be averaged and idealized as being effectively homogenous (a homogenization process in a representative volume element, RVE). Accordingly, the macroscopic constitutive equation of the inhomogeneous solid can be written as

$$\bar{\sigma}_{ij} = \bar{C}_{ijkl}\bar{\varepsilon}_{kl}, \tag{1}$$

where $\bar{C}_{ijkl}$ are the components of the effective stiffness of the solid, and subscripts i, j, k, and l range from 1 to 3. The usual summation convention is adopted for repeated indices in the tensor notation. $\bar{\sigma}_{ij}$ and $\bar{\varepsilon}_{kl}$ are volume-averaged stress and strain tensors, respectively, and defined as

$$\bar{\sigma}_{ij} = \int_V \sigma_{ij} \mathrm{d}^3 \underset{\sim}{x}, \quad \bar{\varepsilon}_{kl} = \int_V \varepsilon_{kl} \mathrm{d}^3 \underset{\sim}{x}, \tag{2}$$

where σ_{ij} and ε_{kl} are stress and strain fields in the RVE, respectively, and are functions of the position vector, $\underset{\sim}{x}$. V is the volume of RVE. It should be noted that the heterogeneous medium and RVE are now interchangeable in the manuscript. If an uniform external loading, $\sigma_{ij}^{\mathrm{ext}}$, is applied to the heterogeneous medium, then $\bar{\sigma}_{ij} = \sigma_{ij}^{\mathrm{ext}}$ by assuming the homogeneous stress boundary conditions. However, the corresponding $\bar{\varepsilon}_{ij}$ has to be obtained through the average of local strain, Eq. (2), such that Eq. (1) can be solved to obtain $\bar{C}_{ijkl}$.

It has been proven, through a variational approach, that the local strain and the strain energy of the heterogeneous system can be evaluated by establishing an equivalent system having a homogeneous reference phase and a distributed effective eigenstrain, ε^0_{ij}, which can be expressed as (Mura, 1987):

$$C^0_{ijkl}\left[\varepsilon_{kl}(\underset{\sim}{x}) - \varepsilon^0_{kl}(\underset{\sim}{x})\right] = C_{ijkl}(\underset{\sim}{x})\varepsilon_{kl}(\underset{\sim}{x}), \tag{3}$$

where $C_{ijkl}(\underset{\sim}{x}) = C^0_{ijkl} + \Delta C_{ijkl}(\underset{\sim}{x})$. C^0_{ijkl} is the stiffness tensor of the reference (homogenous) phase. $\Delta C_{ijkl}(\underset{\sim}{x})$, which characterizes the elastic inhomogeneity, is the stiffness variation from the homogeneity. Once the effective eigenstrain ε^0_{ij} has been obtained, the average strain $\bar{\varepsilon}_{ij}$, the local strain and stress (ε_{ij} and σ_{ij}) can be obtained from the following three coupled equations:

$$\bar{\varepsilon}_{ij} = S^0_{ijkl}\sigma^{\text{ext}}_{kl} + \bar{\varepsilon}^0_{ij}, \tag{4}$$

$$\varepsilon_{ij}(\underset{\sim}{x}) = \bar{\varepsilon}_{ij} + \frac{1}{2}\int_{|\underset{\sim}{\xi}|\neq 0} \frac{(\xi_i\tilde{G}_{jk} + \xi_j\tilde{G}_{ik})\tilde{\sigma}^0_{kl}(\underset{\sim}{\xi})^*\xi_l e^{i\underset{\sim}{\xi}\cdot\underset{\sim}{x}}}{(2\pi)^3} d^3\underset{\sim}{\xi} \tag{5}$$

and

$$\sigma_{ij}(\underset{\sim}{x}) = C^0_{ijkl}\left[\varepsilon_{kl}(\underset{\sim}{x}) - \varepsilon^0_{kl}(\underset{\sim}{x})\right], \tag{6}$$

where $S^0_{ijkl} = C^{0-1}_{ijkl}$ and $\bar{\varepsilon}^0_{ij} = \int_V \varepsilon^0_{ij} d^3(\underset{\sim}{x})$. $\tilde{G}_{jk}$, the components of the Green's function tensor in the Fourier space, are functions of the directional vector, $\underset{\sim}{\xi}$. ξ_i are the components of the directional vector. $\tilde{\sigma}^0_{ij}(\underset{\sim}{\xi})$ is defined as

$$\tilde{\sigma}^0_{ij}(\underset{\sim}{\xi}) = C^0_{ijkl}\int_V \varepsilon^0_{kl}(\underset{\sim}{x})e^{-i\underset{\sim}{\xi}\cdot\underset{\sim}{x}} d^3\underset{\sim}{x}. \tag{7}$$

The * in Eq. (5) denotes the complex conjugate and the integral, $\int_{|\underset{\sim}{\xi}|\neq 0}$, is in the Fourier space excluding the points at $|\xi| = 0$.

Clearly, once the effective eigenstrain ε^0_{ij} is obtained, Eqs. (4–6) should be resolved. This ε^0_{ij} can be determined by either setting the following functional variation, $\delta E^{\text{equiv}}_{\text{elas}}/\delta\varepsilon^0_{ij} = 0$, such that

$$\Delta S_{ijkl}C^0_{klmn}\varepsilon^0_{mn} = \bar{\varepsilon}_{ij} + \frac{1}{2}\int_{|\underset{\sim}{\xi}|\neq 0} \frac{(\xi_i\tilde{G}_{jk} + \xi_j\tilde{G}_{ik})\tilde{\sigma}^0_{kl}(\underset{\sim}{\xi})^*\xi_l e^{i\underset{\sim}{\xi}\cdot\underset{\sim}{x}}}{(2\pi)^3} d^3\underset{\sim}{\xi} \tag{8}$$

or solving the kinetic equations of the phase-field microelasticity defined as (Wang et al., 2002)

$$\frac{\partial\varepsilon^0_{ij}\left(\underset{\sim}{x}, t\right)}{\partial t} = -K_{ijkl}\frac{\delta E^{\text{equiv}}_{\text{elas}}}{\delta\varepsilon^0_{kl}}, \tag{9}$$

where $E^{\text{equiv}}_{\text{elas}}$ is the elastic energy of the equivalent system with the distributed effective eigenstrain ε^0_{ij}; the kinetic coefficient K_{ijkl} is a constant and of no importance as long as it is positive definite; t is the pseudo time. The $E^{\text{equiv}}_{\text{elas}}$ can be expressed as a function of ε^0_{ij}:

$$E^{\text{equiv}}_{\text{elas}} = \frac{1}{2}\int_\Omega C^0_{ijkl}\varepsilon^0_{ij}\varepsilon^0_{kl}\mathrm{d}^3\underset{\sim}{x} + \frac{1}{2}\int_\Omega C^0_{ijkl}\bar{\varepsilon}_{ij}\bar{\varepsilon}_{kl}\mathrm{d}^3\underset{\sim}{x} - \bar{\varepsilon}_{ij}\int_\Omega C^0_{ijkl}\varepsilon^0_{kl}\mathrm{d}^3\underset{\sim}{x} - \frac{1}{2}\int_{|\underset{\sim}{\xi}|\neq 0}\frac{\xi_i\tilde{\sigma}^0_{ij}(\underset{\sim}{\xi})\tilde{G}_{jk}(\underset{\sim}{\xi})\tilde{\sigma}^0_{kl}(\underset{\sim}{\xi})^*\xi_l}{(2\pi)^3}\mathrm{d}^3\underset{\sim}{\xi} + \frac{1}{2}\int_\Omega(-C^0_{ijmn}\,\Delta S_{mnpq}C^0_{pqkl} - C^0_{ijkl})\varepsilon^0_{ij}\varepsilon^0_{kl}\mathrm{d}^3\underset{\sim}{x} \tag{10}$$

with

$$\Delta S_{mnpq} = [C_{mnpq}(\underset{\sim}{x}) - C^0_{mnpq}]^{-1}. \tag{11}$$

Once the effective strain, ε^0_{ij}, is determined using Eq. (9), one can establish the effective stiffness tensor of the heterogeneous material ($\bar{C}_{ijkl}$) through Eqs. (4)–(6) and Eqs. (1) and (2). Thus, the accuracy of the prediction on $\bar{C}_{ijkl}$ highly depends on the preciseness of ε^0_{ij}. In this study, we use the fast Fourier transform (FFT) algorithm for a numerical solution of Eq. (9) since it can provide a quicker convergent solution.

It has been stated in the literature (Wang et al., 2002) that the PFM approach for solutions of ε^0_{ij} is a minimization process of the functional, $E^{\text{equiv}}_{\text{elas}}$. We found that this statement is valid only when the reference (homogeneous) phase is stiffer than the heterogeneous media, namely, $\Delta S_{ijkl}(\underset{\sim}{x})<0$. This can be explained using the second order variation of the elastic energy of the equivalent system, $\delta^2E^{\text{equiv}}_{\text{elas}}$, which is

$$\delta^2E^{\text{equiv}}_{\text{elas}} = -C^0_{ijmn}\Delta S_{mnpq}C^0_{pqkl}. \tag{12}$$

From Eq. (12), if $\Delta S_{ijkl}(\underset{\sim}{x})<0$, then $\delta^2E^{\text{equiv}}_{\text{elas}}>0$. Thus a minimum value of $E^{\text{equiv}}_{\text{elas}}$ can achieve and the argument of minimization process in the literature (Wang et al., 2002) is valid.

On the other hand, for $\Delta S_{ijkl}>0$, $E^{\text{equiv}}_{\text{elas}}$ has a maximum and the solution process cannot be treated as a minimization process. However, solutions of the effective eigenstrain using the PFM approach can be still obtained using the variation of $E^{\text{equiv}}_{\text{elas}}$ with respect to the pseudo time,

$$\frac{\partial E^{\text{equiv}}_{\text{elas}}}{\partial t} = -K_{ijkl}\left(\frac{\delta E^{\text{equiv}}_{\text{elas}}}{\delta\varepsilon^0_{ij}}\right)\left(\frac{\delta E^{\text{equiv}}_{\text{elas}}}{\delta\varepsilon^0_{kl}}\right). \tag{13}$$

From Eq. (13), one can note that $E^{\text{equiv}}_{\text{elas}}$ attains this maximum only if the kinetic coefficient K_{ijkl} is negative definite. Therefore, K_{ijkl} can be either positive or negative definite depending on that if the system has a minimum or maximum of $E^{\text{equiv}}_{\text{elas}}$. The minimum and maximum are contingent upon the stiffness contrast between the heterogeneous media and the reference phase, $C_{mnpq}(\underset{\sim}{x}) - C^0_{mnpq}$. For example, if the reference phase is stiffer than the heterogeneous media, the iterative process for the solution of $\bar{C}_{ijkl}$ in Eq. (1) is a process of decreasing $\bar{C}_{ijkl}$, which corresponds to minimizing the strain energy ($E^{\text{equiv}}_{\text{elas}} = -\sigma^{\text{ext}}_{ij}\sigma^{\text{ext}}_{kl}/2\bar{C}_{ijkl}$ or $E^{\text{equiv}}_{\text{elas}} = \bar{C}_{ijkl}\varepsilon^{\text{ext}}_{ij}\varepsilon^{\text{ext}}_{kl}/2$). On the other hand, if the reference phase is softer than the heterogeneous media, the process is a increasing of $\bar{C}_{ijkl}$, which corresponds to maximizing the strain energy.

It is also worthwhile to note that we can correlate the PFM approach to the Hashin–Shtrikman (H–S) variational principle, which is well known as a powerful tool to provide bounds of effective properties. The functional of the H–S variational approach, Π, is (Hashin and Shtrikman, 1963)

$$\Pi(p_{ij}, \varepsilon_{ij}^{\mathrm{d}}) = \frac{1}{2}\int_V \left(C'_{ijkl}\varepsilon'_{ij}\varepsilon'_{kl} - \Delta C^{-1}_{ijkl} p_{ij} p_{kl} + p_{ij}\varepsilon^{\mathrm{d}}_{ij} + 2p_{ij}\varepsilon'_{ij} \right) \mathrm{d}V, \tag{14}$$

where C'_{ijkl} and ε'_{ij} are the stiffness and strain of a comparison solid (i.e., reference phase), respectively, $\varepsilon^{\mathrm{d}}_{ij} = \varepsilon_{ij} - \varepsilon'_{ij}$, $\Delta C_{ijkl} = C_{ijkl}(\underset{\sim}{x}) - C'_{ijkl}$, $p_{ij} = \Delta C_{ijkl}\varepsilon_{kl}$. The H–S variational statement includes:

(i) the functional Π is stationary (i.e., $\delta\Pi = 0$) if the following equation is satisfied:

$$(C'_{ijkl}\varepsilon^{\mathrm{d}}_{kl})_{,j} + p_{ij,j} = 0, \tag{15}$$

(ii)

$$\begin{aligned} &\delta^2\Pi > 0 \quad \text{if} \quad \Delta C_{ijkl} < 0, \quad \Pi \to \text{Minimum}, \\ &\delta^2\Pi < 0 \quad \text{if} \quad \Delta C_{ijkl} > 0, \quad \Pi \to \text{Maximum}. \end{aligned} \tag{16}$$

If substituting the tensor components of C'_{ijkl}, ε'_{ij}, $\varepsilon^{\mathrm{d}}_{ij}$, and p_{ij} in Eq. (14) of the H–S approach with C^0_{ijkl}, $\bar{\varepsilon}_{ij}$, $\varepsilon_{ij} - \bar{\varepsilon}_{ij}$,and $-C^0_{ijkl}\varepsilon^0_{kl}$ in the PFM approach, respectively, one can notice that Π is identical to the expression of $E^{\mathrm{equiv}}_{\mathrm{elas}}$. However, the PFM approach further provides a kinetic equation to resolve the elastic equilibrium of the heterogeneous media. Consequently, the effective properties can be directly predicted using the PFM approach.

3. Results and discussion

3.1. Accuracy and convergence of the PFM Approach

Figs. 1a–c display the comparison of ε^0_{ij} obtained from the proposed numerical approach with the analytical solutions, where the numerical solution is a function of the number of time step, t^*. One can see, from the figures, that the values of three effective eigenstrains converge to analytical results at $t^* \cong 40$. Although not reported in the figures, there is also good agreement for ε^0_{ij} between the numerical and analytical solutions for a case of shear loading. It is worthwhile to note that the ε^0_{ij} of the medium is zero, while in the void the ε^0_{ij} is uniform and can be analytically obtained from the following equation (Mura, 1987):

$$\varepsilon^0_{ij} = \frac{15(1-v_0)}{7-5v_0} S^0_{ijkl}\sigma^{\mathrm{ext}}_{kl} + \frac{3(1-v_0)(5v_0-1)}{(7-5v_0)(2-4v_0)} S^0_{kkpq}\sigma^{\mathrm{ext}}_{pq}\delta_{ij} \tag{17}$$

with v_0 and S^0_{ijkl} being the Poisson's ratio and compliance of the medium, respectively, and δ_{ij} the identity tensor. Depicted in Fig. 1d is the distribution of normalized stress in the z-axis, σ_{zz}, obtained using the proposed numerical approach, for the medium subjected to a uniform external loading in the z-axis. The color spectrum of σ_{zz} in the figure indicates a stress concentration of 2.03 for $v_0 = 0.3$, which is induced by the inclusion of the void. This value is nearly identical to that of analytical solution: $3(9-5v_0)/2(7-5v_0) = 2.05$.

The PFM approach uses an iterative scheme and FFT algorithms for numerical solutions, which requires iterating on the pseudo-time. Fig. 2 shows the number of iterative

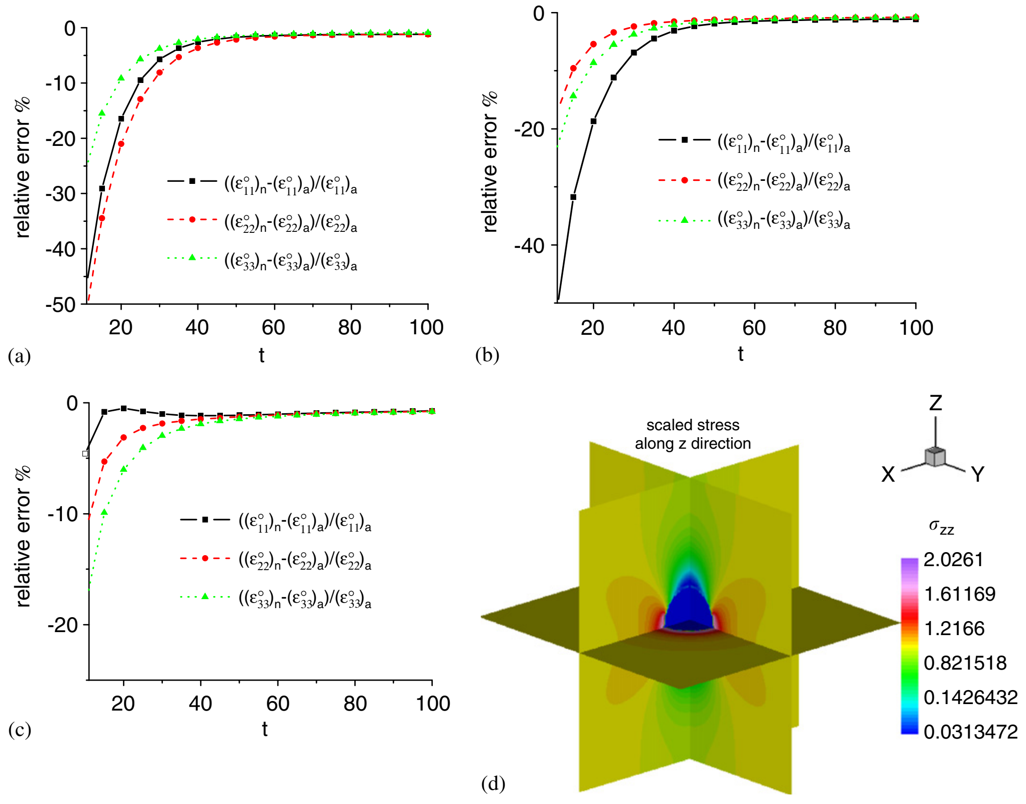

Fig. 1. The relative error of the effective eigenstrains attained from PFM $(\varepsilon^0_{ij})_n$ and analytical solutions $(\varepsilon^0_{ij})_a$ as a function of time step, t^* ($t^* = t/\Delta t$, $\Delta t = 0.1$), for a spherical cavity embedded in an infinite isotropic elastic medium ($v_0 = 0.3$) under different external loadings: a uniaxial stress state along z-axis (a); an equal-biaxial stress state along y- and z-axes (b); an equal-triaxial stress state (c) A spectrum of scaled stress ($\sigma_{zz}/\sigma_{zz}^{\text{ext}}$) distribution of case (a) is shown in (d). The computational grid of RVE considered in all the numerical examples is $128 \times 128 \times 128$, unless specified.

time required to attain the convergent solution, for an infinite isotropic elastic medium with a spherical inclusion under uniaxial loading, as a function of stiffness contrast between the inclusion and matrix Fig. 3a gives a stress component in the void phase obtained from the PFM approach as a function of t^* for a 3D porous medium with three different microstructures (porosity $= 0.4$) under a uniaxial loading. For all the microstructures studied, one can see from the figure that the stress component in the loading direction, $\bar{\sigma}_{zz}$, converges to zero at similar rates. From the results shown in Figs. 2 and 3, one can conclude that the convergence of the PFM approach is not sensitive to the microstructural geometry and the stiffness contrast between constituents. This is quite different from what was reported in some FFT-based approaches (e.g., Moulinec and Suquet, 1994; Müller, 1996; Moulinec and Suquet, 1998; Michel et al., 1999; Eyre and Milton, 1999), in which such a sensitivity has been observed. In the PFM approach, the iterative scheme uses the Ginzburg–Landau kinetic equation where the effective eigenstrain is taken as a non-conserved phase field variable, and the convergence is driven by

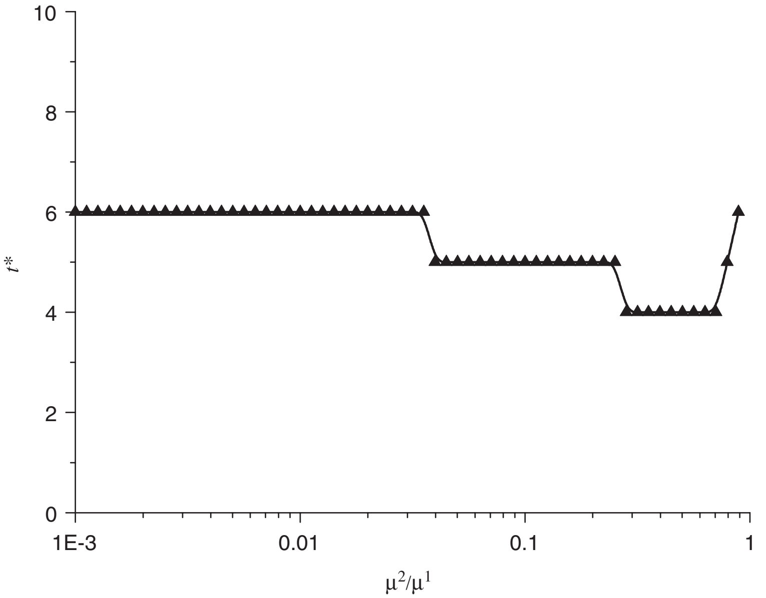

Fig. 2. The number of iterative time step required to attain convergence as a function of phase contrast, μ_2/μ_1; μ_2 and μ_1 are the shear moduli of the inclusion and matrix, respectively. It was assumed that the convergence was achieved when the relative error of the effective eigenstrains between PFM $(\varepsilon_{ij}^0)_n$ and analytical solutions $(\varepsilon_{ij}^0)_{\rm a}$ was less than 1%. $\Delta t = 0.4(1 - \mu_2/\mu_1)^{1.2}$.

monotonically decreasing (or increasing) the elastic energy of the equivalent system in Eq. (9) so that a convergent solution is obtained efficiently.

3.2. Application of PFM approach to heterogeneous media

Moreover, we applied the proposed approach to a two-phase composite for predicting its effective elastic properties. This composite consisted of identical spherical inclusions with radius, R, in a periodic cubic arrangement, Fig. 4a. Both the matrix and inclusion were assumed to be isotropic. This composite with cubic geometric symmetry results in three independent elastic constants (Ting, 1996). Figs. 4b–d present the comparison of three elastic constants obtained from the current approach with those reported from literature (Iwakuma and Nemat-Nasser, 1983; Kushch, 1987; Cohen, 2004) as a function of the volume fraction of inclusion, ϕ. The results in the figures indicate excellent agreement between the current approach and other analytical approaches for the volume fraction considered ($0<\phi<0.5$). This further demonstrates the accuracy of the current approach. In this study $\phi = 4\pi R^3/3l^3$, with l being the distance between the centers of adjacent inclusions. By changing R, one can obtain a desired ϕ without causing overlapping of the inclusions.

Figs. 5a and b display the effective shear modulus, $\bar{\mu}$, and bulk modulus, $\bar{k}$, respectively, for the composite with cubic geometric symmetry, Fig. 4a, as a function of ϕ. Besides our current approach, all the results shown in these two figures were obtained from other classic micromechanics approaches (Nemat-Nasser and Hori, 1993), in which the

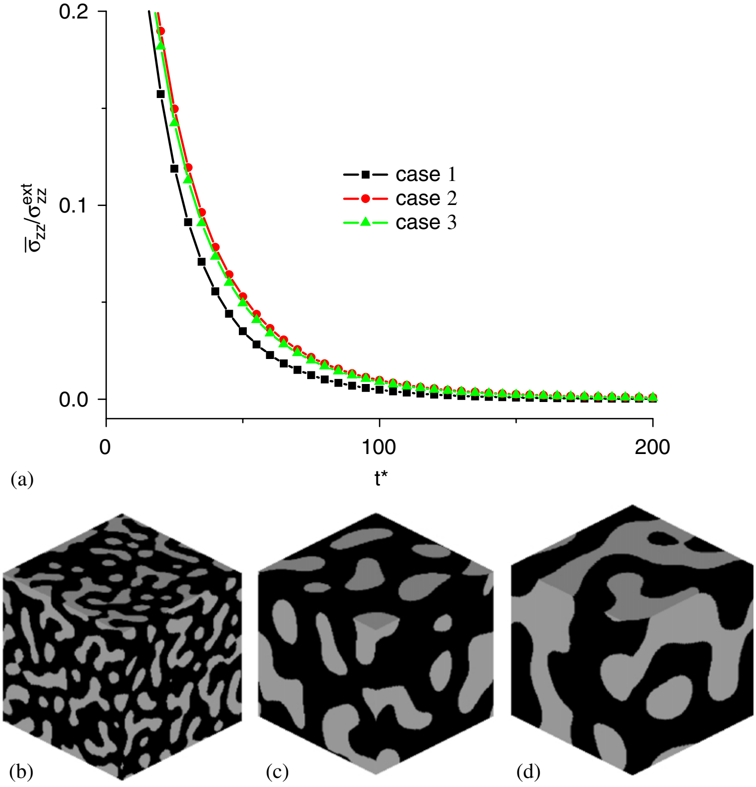

Fig. 3. the scaled average stress component, $\bar{\sigma}_{zz}/\sigma_{zz}^{ext}$, in the void phase versus the number of iterative time step, t^* (a), for three different microstructures, Cases 1–3 (b–d).

two-phase material (Fig. 4a) was assumed to be macroscopically isotropic. Therefore, only two material constants ($\bar{\mu}$ and $\bar{k}$) are listed for comparisons, although the composite is a cubic material and the phase-field approach is valid for general anisotropic materials (micro/macroscopically). From the results in Fig. 5a, for a lower ϕ, there is good agreement on the predictions of the effective shear modulus between the phase-field approach and the micromechanics models considered. However, for a higher ϕ, there is discrepancy on the predictions. A similar trend can also be seen for the predictions of the effective bulk modulus. This is because, for a lower ϕ, the two-phase material in Fig. 4a can be considered as a case of dilute suspension. In other words, the distance between the spherical particles is much larger than their size such that all the interactions between the particles are negligible. Consequently, the assumption of "being macroscopically isotropic" is valid. However, for a higher ϕ, the interaction is more pronounced and the assumption becomes unreasonable. It is worthwhile to note that, based on the agreement in the predictions of bulk modulus between the current approach and Mori–Tanaka method; one can conclude that the interaction of particles has more influence on the shear modulus than the bulk modulus. This is because that, in the Mori–Tanaka method, isotropic interaction between particles was assumed (Mori and Tanaka, 1973). Fig. 5c shows the strength of elastic anisotropy, A, which is obtained from the current method as a

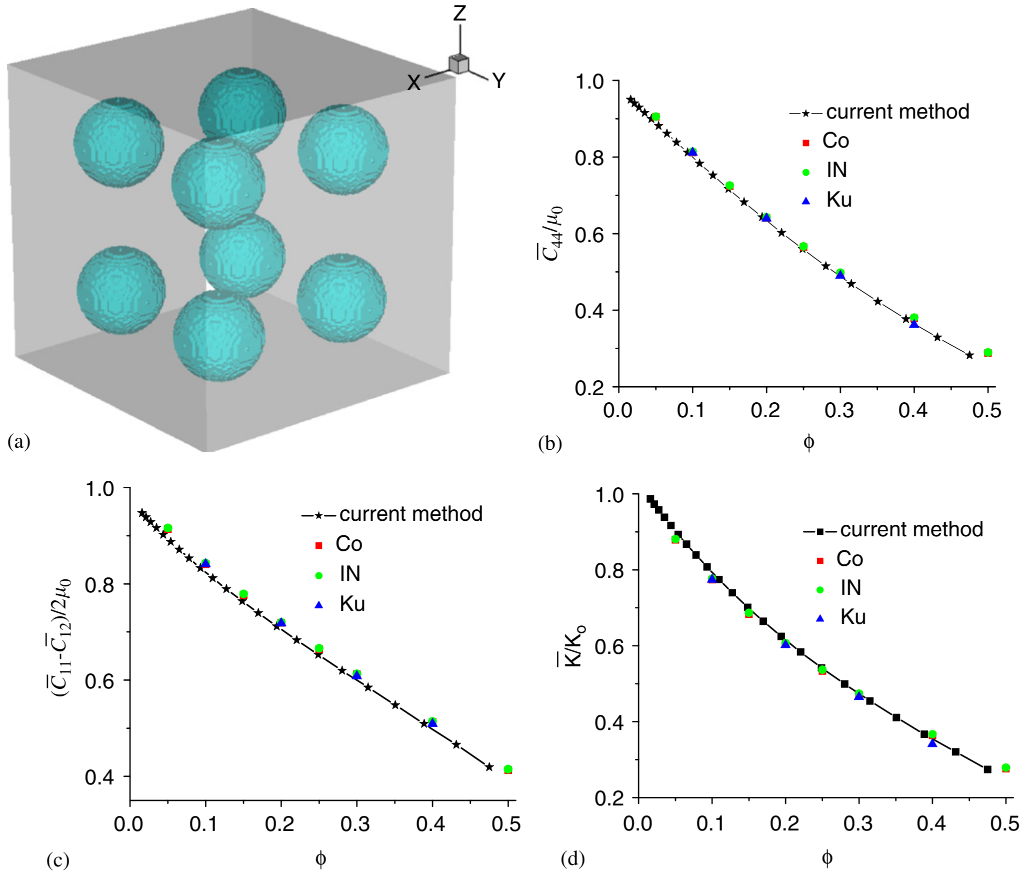

Fig. 4. Periodic microstructure with a simple cubic array of spherical inclusions as indicated in (a), the comparisons of the current method with other methods on the prediction of the effective elastic constants for the cubic array as a function of inclusion volume fraction, ϕ: the effective shear moduli $\bar{C}_{44}$ (b) and $(\bar{C}_{11}-\bar{C}_{12})/2$ (c), the effective bulk modulus $\bar{K}=(\bar{C}_{11}+2\bar{C}_{12})/3$. The other methods are from Cohen (Co) (2004), Iwakuma and Nemat-Nasser (IN) (1983), and Kushch (Ku) (1987). All the reported moduli are scaled with the corresponding moduli of the matrix phase (being the reference phase). The Poisson's ratios of the matrix and inclusion are assumed to be 0.3.

function of ϕ for different stiffness ratios (μ_2/μ_1, where μ_1 and μ_2 are the shear moduli of the matrix and inclusion, respectively). This strength, defined in the figure caption, gives the degree of deviation from the material being macroscopically isotropic ($A = 1.0$). The results in the figure indicate that the degree of anisotropy increases with the decrease of the stiffness ratio (e.g., μ_2 approaches zero, which corresponds to a porous medium), and tends to be one for lower values of ϕ regardless of the stiffness ratio. However, the Eshelby-based approaches considered here do not take the anisotropy into account.

Next, the PFM approach is applied to predict the effective elastic properties of a 3D representation of porous microstructure, Fig. 6a, obtained from X-ray tomography of a tissue scaffold (Chiang et al., 2006). It consists of highly interconnected irregular pore phase, and its matrix phase is assumed to be an isotropic material. The estimate of effective

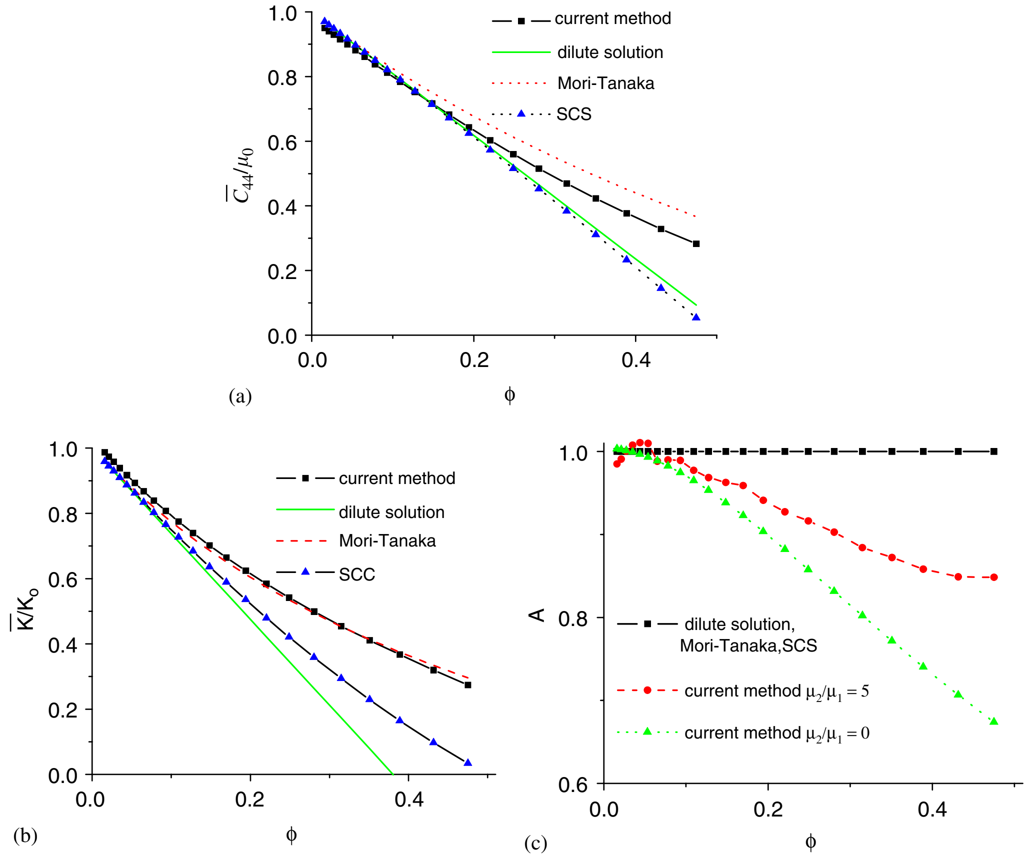

Fig. 5. Comparisons of the current method with some classic micromechanical models on the prediction of the effective elastic constants for the cubic array (Fig. 4a) as a function of inclusion volume fraction: the effective shear modulus $\bar{C}_{44}$ (a), the effective bulk modulus, $\overline{K}$, (c), and the cubic anisotropic strength, A, which is defined as $A = 2\bar{C}_{44}/(\bar{C}_{11} - \bar{C}_{12})$.

stiffness, $\bar{C}_{ijkl}$, from the PFM approach, which is expressed in a contracted notation, $\underset{\sim}{\bar{\mathbf{C}}}$ (Ting, 1996) as follows:

$$\underset{\sim}{\bar{\mathbf{C}}} = \mu_1 \begin{bmatrix} \mathbf{1.109} & \mathbf{0.322} & \mathbf{0.379} & 0.007 & -0.003 & -0.002 \\ \mathbf{0.322} & \mathbf{0.794} & \mathbf{0.328} & 0.025 & -0.005 & -0.017 \\ \mathbf{0.379} & \mathbf{0.328} & \mathbf{1.151} & 0.046 & -0.002 & -0.010 \\ 0.007 & 0.025 & 0.046 & \mathbf{0.307} & -0.007 & 0.001 \\ -0.003 & -0.005 & -0.002 & -0.007 & \mathbf{0.382} & 0.017 \\ -0.002 & -0.017 & -0.010 & 0.001 & 0.017 & \mathbf{0.301} \end{bmatrix} \quad (18)$$

This estimate of Eq. (18) is based on the coordinate system of 3D image in Fig. 6a, which may not be aligned with the symmetry axes of the material. Many methods have been developed in order to derive the material symmetry (principal directions) and the corresponding elastic constants using the $\underset{\sim}{\bar{\mathbf{C}}}$ made in an arbitrary coordinate system (e.g.,

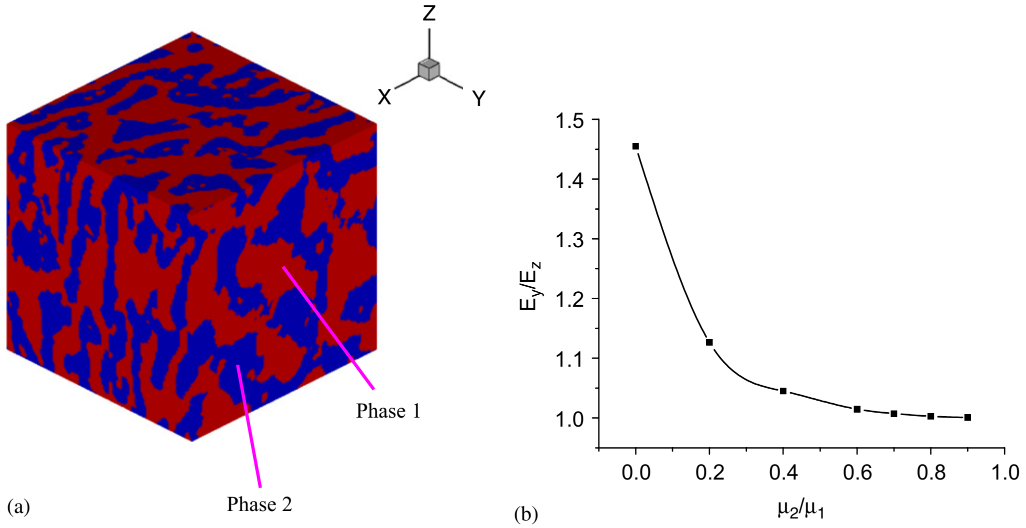

Fig. 6. 3D image of a general two-phase heterogeneous material (100 × 100 × 100) where phase 2 is a pore phase and porosity is 0.45 (a), the degree of anisotropy, defined as the ratio of E_y/E_z, versus the stiffness ratio μ_2/μ_1 (b) with $\upsilon_1 = \upsilon_2 = 0.3$.

Eq. (18)). Since it is beyond the scope of our study to discuss the detailed procedures for the derivation, the interested readers can refer to the literature (Nye, 1957; Cowin and Mehrabadi, 1987; Cowin and Mehrabadi, 1989). We followed the procedure using a fabric-based scheme (Chiang et al., 2006) and found that the image in Fig. 6a macroscopically behaves as a transversely isotropic material, which has a rotational symmetry with respect to the y axes of Fig. 6a. This information reveals that only five independent material constants need to be determined for the stress–strain relations of the material. This transverse isotropy also can be directly observed from the values of components in the matrix $\underset{\sim}{\bar{\mathbf{C}}}$ as (1): the values marked boldly in Eq. (18) are much larger than that of others, such that those non-bold values can be set to zero (2): $\bar{C}_{11} \cong \bar{C}_{33}$, $\bar{C}_{12} \cong \bar{C}_{23}$, $\bar{C}_{44} \cong \bar{C}_{66}$. It is worthwhile to note that our method developed here can predict all the effective elastic constants of the heterogeneous media without knowledge of macroscopic material symmetry.

The calculation of the components in $\underset{\sim}{\bar{\mathbf{C}}}$ was achieved by applying a load to the heterogeneous medium six times. Each time, the load is introduced in such a way corresponding to a certain component of stress in the contracted notation of stress–strain relationship, i.e.,

$$\underset{\sim}{\bar{\varepsilon}} = \underset{\sim}{\bar{\mathbf{C}}}^{-1} \underset{\sim}{\bar{\sigma}}, \tag{19}$$

where $\underset{\sim}{\bar{\varepsilon}}$ and $\underset{\sim}{\bar{\sigma}}$ are the volume-averaged stress and strain. By doing so, one can obtain six equations, and a total of 36 equations will be given for fully effective elastic constants of $\underset{\sim}{\bar{\mathbf{C}}}$ without prior knowledge of material symmetry. One should note that actually only 21 elastic constants are needed at most due to the symmetry of $\underset{\sim}{\bar{\mathbf{C}}}$.

In addition, using the image in Fig. 6a as a general two-phase material case, the effect of the stiffness ratio (μ_2/μ_1) on the type and degree of elastic anisotropy of the material was

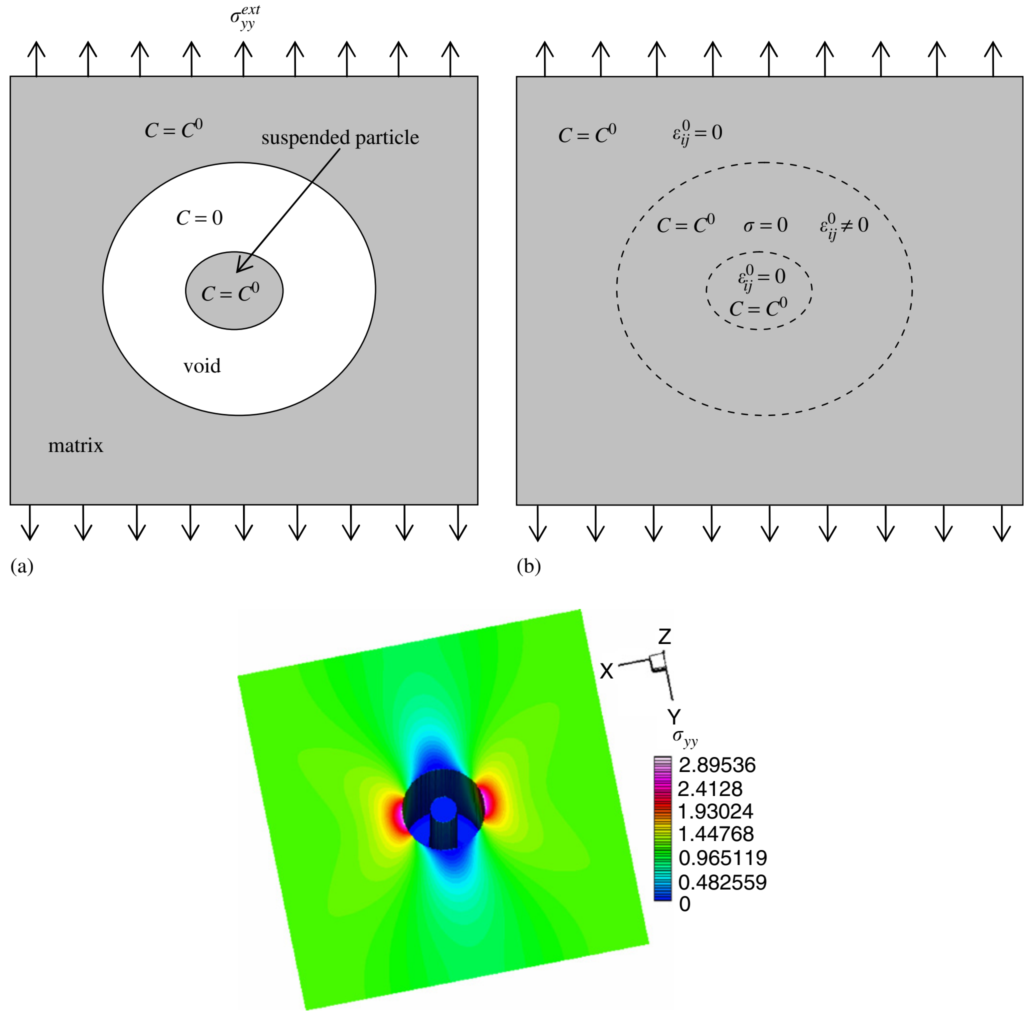

(c)

Fig. 7. 2D schematic of the suspended particle in the circular void embedded in an infinite media under a uniaxial loading σ_{yy}^{ext} (a), the equivalent homogeneous system with the elastic moduli, C_{ijkl}^0, and the effective eigenstrain, ε_{ij}^0, (b), the scaled stress ($\sigma_{yy}/\sigma_{yy}^{\text{ext}}$) distribution (c).

examined by the current approach. For all the stiffness ratios considered ($0.0 < \mu_2/\mu_1 < 1.0$ while ϕ remains constant), the aforementioned transverse isotropy with the principal directions aligned to the reference coordinates is sustained. This indicates that the principal directions of the material remain unchanged. However, the strength of anisotropy, $\overline{E}_y/\overline{E}_z$, changes as a function of the stiffness ratio (Fig. 6b). $\overline{E}_y$ and $\overline{E}_z$ are effective elastic moduli in y and z directions, respectively. These results imply that the elastic symmetries, if they exist, are only functions of microstructural geometry of the material, while the strength of anisotropy of the material is dependent not only on the microstructural geometry but also on the stiffness ratio of the constituents, which are consistent with our recent predictions using a fabric-based scheme (Chiang et al., 2006).

Often, in complex porous media, suspended solid inclusions can be found in interconnected pore channels. For example, incompletely sintered grain is a common morphology in porous ceramics (Roberts and Garboczi, 2000); residual particles are met in porous scaffolds in tissue engineering (Hutmacher, 2000). These suspended inclusions cause computational singularities during numerical solutions to the governing equations, which predict the responses of physical systems subjected to external influences. However, the current approach in this study, adapting the concept of the equivalent inclusion, can avoid the numerical singularity and also give accurate predictions for the stress–strain relations. This can be explained using a 2D configuration in Fig. 7, which indicates that the elastic equilibrium state of the inhomogeneous porous media with a suspended inclusion (Fig. 7a) is identical to that of the equivalent homogeneous media with the effective eigenstrain (Fig. 7b). Since the equivalent system is in an elastic equilibrium state, the stress and strain in the region covered by pore phase is zero, and the values of the effective eigenstrains in the suspended particle are zero. As a result, the stress-free state of suspended inclusion is automatically satisfied. Fig. 7c illustrates the spectrum of local stress field in the loading direction (σ_{yy}). The result in the figure indicates that a stress-free state does exist in the suspended particle and a stress concentration of 2.895 incurred due to the existence of a circular void, which is very close to 3.0 of the analytical solution. This confirms that our approach, based on phase-field theory, provides not only the accurate effective mechanical properties but also the local stress field. In many application cases, both the overall mechanical properties of the heterogeneous media and the local stress (or strain) field in the media play equivalent important roles. For example, in tissue engineering the porous scaffold is used to guide cell proliferation and tissue growth. A desirable scaffold should provide enough effective stiffness and support more uniform growth of cells, which is mediated by the local stresses. Although it is beyond the scope of our study, the PFM approach can also be extended to predict inelastic properties of heterogeneous media. For the inelastic response, inelastic strain, $\varepsilon_{ij}^{\mathrm{p}}(\underset{\sim}{x})$, can be introduced as an extra phase-field variable additional to $\varepsilon_{ij}^{0}(\underset{\sim}{x})$ in the effective eigenstrain of PFM approach, namely, $\varepsilon'^{0}_{ij}(\underset{\sim}{x}) = \varepsilon_{ij}^{0}(\underset{\sim}{x}) + \varepsilon_{ij}^{\mathrm{p}}(\underset{\sim}{x})$. $\varepsilon_{ij}^{\mathrm{p}}$ should obey similar kinetic equations (i.e., Eq. (9)) expressed for elastic media, except the functional being dissipative potential rather than elastic potential.

4. Conclusions

We have adapted the phase-field microelasticity method into the homogenization process to estimate all the effective elastic constants of 3D heterogeneous (multiphase) materials with both intermingled and dispersed phases. The PFM method is based on the Eshelby effective eigenstrain approach and the incorporation of the phase-field theory for attaining the eigenstrain. Our results indicate that such incorporation of the phase-field microelasticity in the homogenization process can give accurate prediction of the elastic constants and local deformation of heterogeneous media. We have also demonstrated that, by adapting the concept of the equivalent inclusion, one can avoid the numerical singularity to obtain the proper local stress–strain relations for complex porous media with suspended inclusions. In addition, this study has shown that PFM approach and the Hashin–Shtrikman (H–S) variational principle have likeliness in the expression for elastic energy of the equivalent system. The PFM approach predicts the effective properties of heterogeneous media while the H–S approach can only provide bounds of effective properties. Although, two-phase heterogeneous medium, with both phases being homogeneous and linear isotropic materials, were examined in the study, the current method is applicable to the multiphase medium with their constituents being anisotropic materials.

References

Bilger, N., Auslender, F., Bornert, M., Michel, J.C., Moulinec, H., Suquet, P., Zaoui, A., 2005. Effect of a nonuniform distribution of voids on the plastic response of voided materials: a computational and statistical analysis. Int. J. Solids Strut. 42, 517–538.

Budiansky, B., 1965. On the elastic moduli of some heterogeneous materials. J. Mech. Phys. Solids 13, 223–227.

Chiang, M.Y.M., Wang, X.F., Landis, F.A., Joy, D., Snyder, C.R., 2006. Quantifying the directional parameter of structural anisotropy in porous media. Tissue Eng. 12, 1–10.

Christensen, R.M., 1979. Mechanics of Composite Materials. Wiley, New York.

Christensen, R.M., Lo, K.H., 1979. Solutions for effective shear properties in three phase sphere and cylinder models. J. Mech. Phys. Solids 27, 315–330.

Cohen, I., 2004. Simple algebraic approximations for the effective elastic moduli of cubic arrays of spheres. J. Mech. Phys. Solids 52, 2167–2183.

Cowin, S.C., Mehrabadi, M.M., 1987. On the identification of material symmetry for anisotropic elastic-materials. Quart. J. Mech. Appl. Math. 40, 451–476.

Cowin, S.C., Mehrabadi, M.M., 1989. Identification of the elastic symmetry of bone and other materials. J. Biomech. 22, 503–515.

Cowin, S.C., 1999. Bone poroelasticity. J. Biomech. 32, 217–238.

Eshelby, J.D., 1957. The determination of the elastic field of an ellipsoidal inclusion, and related problems. Proc. R. Soc. Lond. A 241, 376–396.

Eyre, D.J., Milton, G.W., 1999. A fast numerical scheme for computing the response of composites using grid refinement. Eur. Phys. J. AP 6, 41–47.

Hashin, Z., Shtrikman, S., 1963. A variational approach to the theory of the elastc behavior of multiphase materials. J. Mech. Phys. Solids 11, 127–140.

Hill, R., 1965. A self-consistent mechanics of composite materials. J. Mech. Phys. Solids 13, 213–222.

Hollister, S.J., 2005. Porous scaffold design for tissue engineering. Nature Mater. 4, 518–524.

Hutmacher, D.W., 2000. Scaffolds in tissue engineering bone and cartilage. Biomaterials 21, 2529–2543.

Idiart, M.I., Moulinec, H., Castrañeda, P.P., Suquet, P., 2006. Macroscopic behavior and field fluctuations in viscoplastic composites: second-order estimates versus full-field simulations. J. Mech. Phys. Solids 54, 1029–1063.

Iwakuma, T., Nemat-Nasser, S., 1983. Composites with periodic microstructure. Comput. Struct. 16, 13–19.

Kouznetsova, V., Brekelmans, W.A.M., Baaijens, F.P.T., 2001. An approach to micro–macro modeling of heterogeneous materials. Comput. Mech. 27, 37–48.

Kröner, E., 1977. Bounds for effective elastic-moduli of disordered materials. J. Mech. Phys. Solids 25, 137–155.

Kushch, V.I., 1987. Computaion of the effective elastic moduli of a granular composite material of regular structure. Sov. Appl. Mech. 23, 362–365.

Kushch, V.I., 1998. Interacting cracks and inclusions in a solid by multipole expansion method. Int. J. Solids Struct. 35, 1751–1762.

Martin, R.B., 1991. Determinations of the mechanical properties of bones. J. Biomech. 24, 79–88.

McLaughlin, R., 1977. A study of the differential scheme for composite materials. Int. J. Eng. Sci. 15, 237–244.

Michel, J.C., Moulinec, H., Suquet, R., 1999. Effective properties of composite materials with periodic microstructure: a computational approach. Comput. Methods Appl. Mech. Eng. 172, 109–143.

Moulinec, H., Suquet, P., 1994. A fast numerical method for computing the linear and nonlinear properties of composites. C. R. Acad. Sci. Paris II 318, 1417–1423.

Moulinec, H., Suquet, P., 1998. A numerical method for computing the overall response of nonlinear composites with complex microstructure. Comput. Methods Appl. Mech. Eng. 157, 69–94.

Mori, T., Tanaka, K., 1973. Average stress in the matrix and average elastic energy of materials with misfitting inclusions. Acta Metallogr. 21, 571–574.

Müller, W.H., 1996. Mathematical versus experimental stress analysis of inhomogeneities in solids. J. Phys. IV 6, C1-139–C1-148.

Mura, T., 1987. Micromechanics of Defects in Solids. Kluwer, Dordrecht.

Nunan, K.C., Keller, J.B., 1984. Effective elasticity tensor of a periodic composite. J. Mech. Phys. Solids 32, 259–280.

Nemat-Nasser, S., Hori, M., 1993. Micromechanics: Overall Properties of Heterogeneous Materials. North-Holland, Amsterdam.

Nemat-Nasser, S., Taya, M., 1981. On effective moduli of an elastic body containing periodically distributed voids. Quart. Appl. Math. 39, 43–59.

Nemat-Nasser, S., Iwakuma, T., Hejazi, M., 1982. On composite with periodic structure. Mech. Mater. 1, 239–267.

Nye, J.F., 1957. Physical Properties of Crystals: Their Representation by Tensors and Matrices. Oxford, Clarendon.

Roberts, A.P., Garboczi, E.J., 2000. Elastic properties of model porous ceramics. J. Am. Ceram. Soc. 83, 3041–3048.

Sanchez-Palencia, E., Zaoui, A. (Eds.), 1987. Homogenization Techniques for Composite Media. Lecture Notes in Physics, vol. 272. Springer, Berlin.

Sangani, A.S., Lu, W., 1987. Elastic coefficients of a composite containing spherical inclusions in a periodic array. J. Mech. Phys. Solids 35, 1–21.

Sun, W., Starly, B., Nam, J., Darling, A., 2005. Bio-CAD modeling and its applications in computer-aided tissue engineering. Comput.-Aided Des. 37, 1097–1114.

Ting, T.C.T., 1996. Anisotropic Elasticity: Theory and Applications. Oxford University Press, New York.

Torquato, S., 1997. Effective stiffness tensor of composite media I. Exact series expansions. J. Mech. Phys. Solids 45, 1421–1448.

Torquato, S., 1998. Effective stiffness tensor of composite media: II. Applications to isotropic dispersions. J. Mech. Phys. Solids 46, 1411–1440.

Torquato, S., 2002. Random Heterogeneous Materials: Microstructure and Macroscopic Properties. Springer, New York.

Turner, C.H., Cowin, S.C., Rho, J.Y., Ashman, R.B., Rice, J.C., 1990. The fabric dependence of the orthotropic elastic constants of cancellous bone. J. Biomech. 23, 549–561.

Wang, Y.U., Jin, Y.M.M., Khachaturyan, A.G., 2002. Phase field microelasticity theory and modeling of elastically and structurally inhomogeneous solid. J. Appl. Phys. 92, 1351–1360.

Wegner, L.D., Gibson, L.J., 2000. The mechanical behaviour of interpenetrating phase composites—I: modeling. Int. J. Mech. Sci. 42, 925–942.

Willis, J.R., 1977. Bounds and self-consistent estimates for the overall moduli of anisotropic composites. J. Mech. Phys. Solids 25, 185–202.

Zheng, Q.S., Du, D.X., 2001. An explicit and universally applicable estimate for the effective properties of multiphase composites which accounts for inclusion distribution. J. Mech. Phys. Solids 49, 2765–2788.